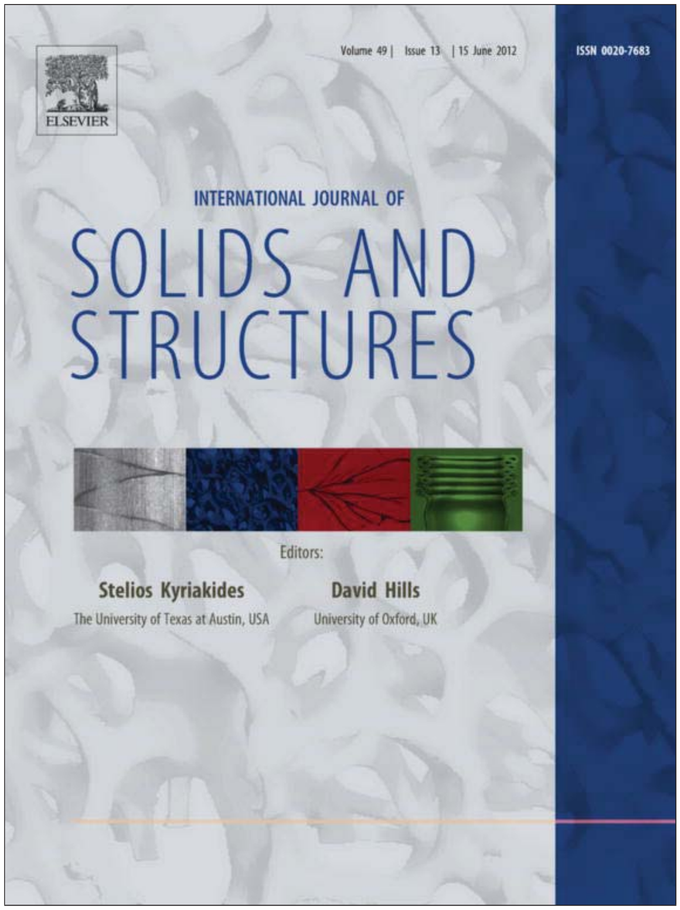
Volume 49 | Issue 13 | 15 June 2012
ISSN 0020-7683
ELSEVIER
INTERNATIONAL JOURNAL OF
SOLIDS AND
STRUCTURES
Editors:
Stelios Kyriakides
The University of Texas at Austin, USA
David Hills
University of Oxford, UK

International Journal of Solids and Structures 49 (2012) 1773–1785

Contents lists available at SciVerse ScienceDirect

International Journal of Solids and Structures

journal homepage: www.elsevier.com/locate/ijsolstr

Inclusion of arbitrary polygon with graded eigenstrain in an anisotropic piezoelectric full plane

L.G. Sun [a], K.Y. Xu [a,*], E. Pan [b,c,*]

[a] Shanghai Institute of Applied Mathematics and Mechanics, Shanghai Key Laboratory of Mechanics in Energy Engineering, Department of Mechanics, Shanghai University, Shanghai 200072, China
[b] The School of Mechanical Engineering, Zhengzhou University, Zhengzhou, Henan 450001, China
[c] Department of Civil Engineering, The University of Akron, OH 44325-3905, USA

ARTICLE INFO

Article history:
Received 2 December 2011
Received in revised form 7 March 2012
Available online 6 April 2012

Keywords:
Eshelby problem
Polygonal inclusion
Graded eigenstrain
Electromechanical coupling
Green's function

ABSTRACT

In this paper, an exact closed-form solution for the Eshelby problem of a polygonal inclusion with a graded eigenstrain in an anisotropic piezoelectric full plane is presented. For this electromechanical coupling problem, by virtue of Green's function solutions, the induced elastic and piezoelectric fields are first expressed in terms of line integrals on the boundary of the inclusion. Using the line-source Green's function, the line integral is then carried out analytically for the linear eigenstrain case, with the final expression involving only elementary functions. Finally, the solution is applied to the semiconductor quantum wire (QWR) of square, triangle, circle and ellipse shapes within the GaAs (001) substrate. It is demonstrated that there exists significant difference between the induced field by the uniform eigenstrain and that by the linear eigenstrain. Since the misfit eigenstrain in most QWR structures is actually non-uniform, the present solution should be particularly appealing to nanoscale QWR structure analysis where strain and electric fields are coupled and are affected by the non-uniform misfit strain.

1. Introduction

Eshelby problem (Eshelby, 1957, 1961) is the subject of constant studies (Mura, 1987) and has numerous applications in heterogeneous materials (composites, polycrystalline materials etc.). Some recent studies include the effective elastoplastic behavior of composites (Ju and Sun, 2001) and dynamic Eshelby tensor in ellipsoidal inclusions (Michelitsch et al., 2003). While most Eshelby problems associated with isotropic elasticity can be solved analytically for both 2D- and 3D-deformations (Kouris and Mura, 1989; Rodin, 1996; Gao and Ma, 2010), the corresponding problems in anisotropic elasticity usually require numerical solution (Dong et al., 2003), except perhaps for the transversely isotropic elasticity case, for which an analytical solution can be obtained (Yu et al., 1994).

Inclusion of an arbitrary shape is particularly useful in the study of strained semiconductor quantum devices (Freund and Gosling, 1995; Davies, 1998; Andreev et al., 1999). It should be also noted that most semiconductor materials are piezoelectric, with some of them being strongly electromechanically coupled (Pan, 2002a,b). Under the assumption of isotropic elasticity with uniform eigenstrain, analytical solutions can be obtained for the inclusion with a polygonal shape (Rodin, 1996; Nozaki and Taya, 1997; Glas, 2002a,b). Ru (1999, 2000) extended the isotropic elasticity to the corresponding anisotropic elasticity and piezoelectricity by using the special conformal mapping method. While the conformal mapping method is elegant and convenient for the inclusion with smooth boundary, it could be inefficient for the general polygonal shape since the conformal mapping function may involve infinite terms. An alternative to the conformal mapping method is the Green's function method (Pan, 2004; Sun et al., 2012), which is particularly suited for polygonal shape. Zou et al. (2010) recently proposed a unified approach where both smooth and non-smooth curves can be considered. Also, to handle material anisotropy and arbitrary shape of inclusion, the perturbation method can be applied (Wang and Chu, 2006; Chu et al., 2011). On the other hand, some research work has been done for spherical and circular inclusions in a finite domain (Li et al., 2005, 2007). So the problem of polygonal inclusion in a finite anisotropic piezoelectric domain should be a challenging work.

An inclusion under non-uniform eigenstrain is very common, particularly in the strained QWR due to the misfit lattice. For a non-uniform eigenstrain problem, Eshelby (1961) showed that if the eigenstrain inside an ellipsoidal inclusion is in the form of a polynomial in Cartesian coordinates, then the induced strain field in the inclusion is also characterized by a polynomial of the same order. Only a few Eshelby inclusion problems have been solved for the non-uniform eigenstrain case so far. This includes the inclusion problem for ellipsoids with non-uniform dilatational Gaussian

* Corresponding authors.
E-mail addresses: kyxu@shu.edu.cn (K.Y. Xu), pan2@uakron.edu (E. Pan).

0020-7683/$ - see front matter © 2012 Elsevier Ltd. All rights reserved.
http://dx.doi.org/10.1016/j.ijsolstr.2012.03.039

and exponential eigenstrains (Sharma and Sharma, 2003); the isotropic ellipsoidal inclusion with polynomial eigenstrains (Rahman, 2002); and recently, elliptic inhomogeneity problem due to linear and polynomial distributions of eigenstrain (Nie et al., 2007; Guo et al., 2011). However, the corresponding arbitrarily shaped inclusion with non-uniform eigenstrain problem remains to be solved.

Thus, in this paper, we present an exact closed-form solution for an arbitrarily shaped polygonal inclusion in anisotropic piezoelectric full-planes where the inclusion is under a linear eigenstrain field. We first express the induced elastic and piezoelectric fields in terms of a line integral on the boundary of the inclusion, with the integrand being the multiplication of the line-source Green's function and the equivalent body force of the piezoelectric solid. The line integral is then carried out analytically on each side of the polygon, with the final results involving only elementary functions. As numerical examples, our solution is applied to the inclusion of square, triangle, circle and ellipse shapes under linear eigenstrains within the GaAs (001) substrate. Our numerical results not only can be used as benchmarks, but also clearly show the effect of linear eigenstrain on the induced field distribution, as compared to the uniform eigenstrain case. This paper is organized as follows: In Section 2, we derive the exact-closed form solution for a general polygon under linear eigenstrain in x and z. In Section 3, we apply our solution to a couple of inclusion problems with linear eigenstrains and discuss certain features associated with the induced fields. Conclusions are drawn in Section 4.

2. Proposed method and solution

Let us assume that there is an extended general eigenstrain γ^*_{Ij} (i.e., the eigenstrain γ^*_{ij} and the eigen-electric field E^*_j) within the QWR domain V bounded by its surface ∂V (Fig. 1), with V being embedded in an infinite substrate. The extended eigenstrain is further assumed to be a linear function of the coordinates (x, z). Our task is to find the eigenstrain-induced field within the QWR and its surrounding substrate.

For a general eigenstrain γ^*_{Ij} at $\boldsymbol{x} = (x, z)$ within domain V, the induced extended displacement at $\boldsymbol{X} = (X, Z)$ can be found via the method of superposition. In other words, the response is an integral, over V, of the equivalent body force in the square bracket below, multiplied by the line-source Green's function (Pan, 2004), i.e.,

$$u_K(\boldsymbol{X}) = -\int_V u^K_J(\boldsymbol{x};\boldsymbol{X})[C_{iJLm}\gamma^*_{Lm}(\boldsymbol{x})]_{,i}\,\mathrm{d}V(\boldsymbol{x}) \tag{1}$$

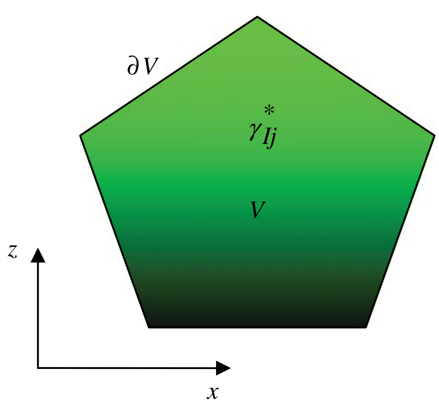

Fig. 1. An arbitrary QWR domain V bounded by ∂V under a linear eigenstrain γ^*_{Ij} (γ^*_{ij} and $-E^*_j$). The misfit eigenstrain is a linear function of the coordinates (x, z), and the QWR is in a general anisotropic piezoelectric infinite substrate.

where $u^K_J(x;\boldsymbol{X})$ is the Jth Green's elastic displacement/electric potential at $\boldsymbol{x}$ due to a line-force/line-charge in the K-th direction applied at $\boldsymbol{X}$.

Integrating by parts and noticing that the eigenstrain is nonzero only in V, Eq. (1) can be written alternatively as

$$u_K(\boldsymbol{X}) = \int_V u^K_{J,x_i}(\boldsymbol{x};\boldsymbol{X})C_{iJLm}\gamma^*_{Lm}(\boldsymbol{x})\,\mathrm{d}V(\boldsymbol{x}) \tag{2}$$

We assume that within the QWR domain V, the eigenstrain can be expressed as a linear function of the coordinates (x,z):

$$\gamma^*_{Lm}(\boldsymbol{x}) = \gamma^{*0}_{Lm} + \gamma^{*x}_{Lm}x + \gamma^{*z}_{Lm}z \tag{3}$$

Thus, Eq. (2) becomes

$$u_K(\boldsymbol{X}) = \int_V u^K_{J,x_i}(\boldsymbol{x};\boldsymbol{X})C_{iJLm}[\gamma^{*0}_{Lm} + \gamma^{*x}_{Lm}x + \gamma^{*z}_{Lm}z]\,\mathrm{d}V(\boldsymbol{x}) \tag{4}$$

or,

$$u^0_K(\boldsymbol{X}) + u^x_K(\boldsymbol{X}) + u^z_K(\boldsymbol{X}) \equiv \int_V u^K_{J,x_i}(\boldsymbol{x};\boldsymbol{X})[C_{iJLm}\gamma^{*0}_{Lm} + C_{iJLm}\gamma^{*x}_{Lm}x + C_{iJLm}\gamma^{*z}_{Lm}z]\,\mathrm{d}V(\boldsymbol{x}) \tag{5}$$

where the superscripts 0, x, z denote the terms corresponding, respectively, to the eigenstrains which are uniform, linear in x, and linear in z. We now discuss these terms one by one below.

(1) The first integration is associated with a uniform eigenstrain field that was well studied. For example, based on Pan (2004), this area integral can be easily transformed to the following boundary integration

$$u^0_K(\boldsymbol{X}) = C_{iJLm}\gamma^{*0}_{Lm}\int_{\partial V} u^K_J(\boldsymbol{x};\boldsymbol{X})n_i(\boldsymbol{x})\,\mathrm{d}S(\boldsymbol{x}) \tag{6}$$

where $n_i(\boldsymbol{x})$ is the outward normal on the boundary ∂V of the QWR.

(2) The second integration is associated with a linear eigenstrain field in x, which is expressed as

$$u^x_K(\boldsymbol{X}) = \int_V u^K_{J,x_i}(\boldsymbol{x};\boldsymbol{X})[C_{iJLm}\gamma^{*x}_{Lm}x]\,\mathrm{d}V(\boldsymbol{x}) \tag{7}$$

By separating the two derivative terms, we have

$$u^x_K(\boldsymbol{X}) = \int_V \{u^K_{J,x}(\boldsymbol{x};\boldsymbol{X})[C_{xJLm}\gamma^{*x}_{Lm}x] + u^K_{J,z}(\boldsymbol{x};\boldsymbol{X})[C_{zJLm}\gamma^{*x}_{Lm}x]\}\,\mathrm{d}V(\boldsymbol{x}) \tag{8}$$

which can be further transformed to the boundary integrals as

$$u^x_K(\boldsymbol{X}) = C_{iJLm}\gamma^{*x}_{Lm}\int_{\partial V} u^K_J(\boldsymbol{x};\boldsymbol{X})xn_i(\boldsymbol{x})\,\mathrm{d}S(\boldsymbol{x}) - C_{xJLm}\gamma^{*x}_{Lm} \times \int_{\partial V} U^{xK}_J(\boldsymbol{x};\boldsymbol{X})n_x(\boldsymbol{x})\,\mathrm{d}S(\boldsymbol{x}) \tag{9}$$

(3) The third integration is associated with a linear eigenstrain field in z, expressed as

$$u^z_K(\boldsymbol{X}) = \int_V u^K_{J,x_i}(\boldsymbol{x};\boldsymbol{X})[C_{iJLm}\gamma^{*z}_{Lm}z]\,\mathrm{d}V(\boldsymbol{x}) \tag{10}$$

Similarly, it can be written as a summation of the following two terms

$$u^z_K(\boldsymbol{X}) = \int_V \{u^K_{J,x}(\boldsymbol{x};\boldsymbol{X})[C_{xJLm}\gamma^{*z}_{Lm}z] + u^K_{J,z}(\boldsymbol{x};\boldsymbol{X})[C_{zJLm}\gamma^{*z}_{Lm}z]\}\,\mathrm{d}V(\boldsymbol{x}) \tag{11}$$

which can be further transformed to the boundary integrals as

$$u^z_K(\boldsymbol{X}) = C_{iJLm}\gamma^{*z}_{Lm}\int_{\partial V} u^K_J(\boldsymbol{x};\boldsymbol{X})zn_i(\boldsymbol{x})\,\mathrm{d}S(\boldsymbol{x}) - C_{zJLm}\gamma^{*z}_{Lm} \times \int_{\partial V} U^{zK}_J(\boldsymbol{x};\boldsymbol{X})n_z(\boldsymbol{x})\,\mathrm{d}S(\boldsymbol{x}) \tag{12}$$

In Eqs. (9) and (12), the two new functions are defined as

Table 1
Induced stress component σ_{xx} (GPa) in both the circular inclusion and matrix of GaAs (001). The circular inclusion has a radius r = 10 nm and the eigenstrain inside is linear in x-direction, i.e., $\gamma^{*0}_{Lm}=0$, $\gamma^{*x}_{xx}=\gamma^{*x}_{zz}=0.07$, $\gamma^{*z}_{Lm}=0$. The circle is approximated by the N-sided polygon (N = 10, 20, 40, 60, 80, and 100).

X = Z (nm)	N = 10	N = 20	N = 40	N = 60	N = 80	N = 100
1	−0.64646	−0.64734	−0.64734	−0.64734	−0.64734	−0.64734
2	−1.29298	−1.29467	−1.29468	−1.29468	−1.29468	−1.29468
3	−1.93770	−1.94198	−1.94202	−1.94202	−1.94202	−1.94202
4	−2.58044	−2.58911	−2.58935	−2.58935	−2.58937	−2.58935
5	−3.22172	−3.23537	−3.23668	−3.23664	−3.23669	−3.23667
6	−3.81684	−3.87809	−3.88455	−3.88382	−3.88398	−3.88402
7	−8.12927	−7.87522	−4.51451	−4.54046	−4.53344	−4.53229
8	−2.27724	−2.29140	−2.31969	−2.32175	−2.32354	−2.32426
9	−2.08770	−2.14995	−2.17410	−2.17793	−2.17963	−2.18035
10	−1.92260	−1.99685	−2.01891	−2.02274	−2.02437	−2.02505
11	−1.78064	−1.85671	−1.87734	−1.88100	−1.88255	−1.88318
12	−1.65812	−1.73250	−1.75192	−1.75539	−1.75685	−1.75745
13	−1.55135	−1.62283	−1.64119	−1.64447	−1.64586	−1.64642
14	−1.45741	−1.52569	−1.54308	−1.54619	−1.54751	−1.54803
15	−1.37405	−1.43916	−1.45568	−1.45863	−1.45988	−1.46038
16	−1.29955	−1.36164	−1.37737	−1.38018	−1.38137	−1.38185

$$
\begin{aligned}
U_J^{xK}(\boldsymbol{x};\boldsymbol{X})_{,x} &= u_J^K(\boldsymbol{x};\boldsymbol{X})\\
U_J^{zK}(\boldsymbol{x};\boldsymbol{X})_{,z} &= u_J^K(\boldsymbol{x};\boldsymbol{X})
\end{aligned}
\tag{13}
$$

In summary, the induced extended displacement by the linear eigenstrain (3) in the QWR domain V is the summation of the following three boundary integrals on the surface of the QWR:

$$
u_K^0(\boldsymbol{X}) = C_{iJLm}\gamma^{*0}_{Lm}\int_{\partial V} u_J^K(\boldsymbol{x};\boldsymbol{X})n_i(\boldsymbol{x})\,\mathrm{d}S(\boldsymbol{x})
\tag{14}
$$

$$
\begin{aligned}
u_K^x(\boldsymbol{X}) = {} & C_{iJLm}\gamma^{*x}_{Lm}\int_{\partial V} u_J^K(\boldsymbol{x};\boldsymbol{X})xn_i(\boldsymbol{x})\,\mathrm{d}S(\boldsymbol{x}) - C_{xJLm}\gamma^{*x}_{Lm}\\
& \times \int_{\partial V} U_J^{xK}(\boldsymbol{x};\boldsymbol{X})n_x(\boldsymbol{x})\,\mathrm{d}S(\boldsymbol{x})
\end{aligned}
\tag{15}
$$

$$
\begin{aligned}
u_K^z(\boldsymbol{X}) = {} & C_{iJLm}\gamma^{*z}_{Lm}\int_{\partial V} u_J^K(\boldsymbol{x};\boldsymbol{X})zn_i(\boldsymbol{x})\,\mathrm{d}S(\boldsymbol{x}) - C_{zJLm}\gamma^{*z}_{Lm}\\
& \times \int_{\partial V} U_J^{zK}(\boldsymbol{x};\boldsymbol{X})n_z(\boldsymbol{x})\,\mathrm{d}S(\boldsymbol{x})
\end{aligned}
\tag{16}
$$

Therefore, besides the analytical integration derived before for the uniform or constant eigenstrain case (Pan, 2004), the following four analytical integrations are required:

$$
\begin{aligned}
&I_x = \textstyle\int_{\partial V} u_J^K(\boldsymbol{x};\boldsymbol{X})xn_i(\boldsymbol{x})\,\mathrm{d}S(\boldsymbol{x});\ I_z = \int_{\partial V} u_J^K(\boldsymbol{x};\boldsymbol{X})zn_i(\boldsymbol{x})\,\mathrm{d}S(\boldsymbol{x})\\
&J_x = \textstyle\int_{\partial V} U_J^{xK}(\boldsymbol{x};\boldsymbol{X})n_x(\boldsymbol{x})\,\mathrm{d}S(\boldsymbol{x});\ J_z = \int_{\partial V} U_J^{zK}(\boldsymbol{x};\boldsymbol{X})n_z(\boldsymbol{x})\,\mathrm{d}S(\boldsymbol{x})
\end{aligned}
\tag{17}
$$

To carry out these integrals, we assume as before that the boundary of the QWR domain is composed of piecewise straight line segments. We define an arbitrary line segment in the (x,z)-plane starting from point 1 (x_1,z_1) and ending at point 2 (x_2,z_2), in terms of the parameter t $(0\leqslant t\leqslant 1)$, as

$$
\begin{aligned}
x &= x_1 + (x_2 - x_1)t\\
z &= z_1 + (z_2 - z_1)t
\end{aligned}
\tag{18}
$$

Then, the outward normal component $n_i(\boldsymbol{x})$ along the line segment is constant, given by

$$
n_1 = (z_2 - z_1)/l;\ \ n_2 = -(x_2 - x_1)/l
\tag{19}
$$

where $l=\sqrt{(x_2-x_1)^2+(z_2-z_1)^2}$ is the length of the line segment.

Using the exact closed-form expression for the Green's function in the anisotropic piezoelectric full plane, the integration along the line segment for I_x can be easily carried out as:

$$
I_x(\boldsymbol{X}) = n_i\frac{l}{\pi}\mathrm{Im}\{A_{JR}h_R^x(X,Z)A_{KR}\}
\tag{20}
$$

where the Stroh matrix A_{JR} is related to the material property of the substrate (or matrix). Its detailed expression can be found in Pan (2004). Also in Eq. (20), summation from 1 to 4 is implied for the dummy index R.

Function $h_R^x(X,Z)$ and its derivatives (required for the extended strain calculation) are given below:

$$
\begin{aligned}
h_R^x(X,Z) &= \int_0^1 \ln(z_R - s_R)x\,dt\\
&= \frac{x_2-x_1}{4a^2}[a(2b-a) - 2(b^2-a^2)\ln(a+b) + 2b^2\\
&\quad \times \ln(b)] + \frac{x_1}{a}[-a + (a+b)\ln(a+b) - b\ln(b)]
\end{aligned}
\tag{21}
$$

$$
\begin{aligned}
\frac{\partial h_R^x(X,Z)}{\partial X} &= -\frac{x_2-x_1}{a^2}[a - b\ln(\tfrac{a+b}{b})] - \frac{x_1}{a}\ln(\tfrac{a+b}{b})\\
\frac{\partial h_R^x(X,Z)}{\partial Z} &= -\frac{(x_2-x_1)p_R}{a^2}[a - b\ln(\tfrac{a+b}{b})] - \frac{x_1 p_R}{a}\ln(\tfrac{a+b}{b})
\end{aligned}
\tag{22}
$$

where

$$
\begin{aligned}
a &= (x_2 - x_1) + p_R(z_2 - z_1)\\
b &= (x_1 + p_R z_1) - s_R
\end{aligned}
\tag{23}
$$

$$
z_R = x + p_R z;\ s_R = X + p_R Z
\tag{24}
$$

with p_R (R = 1, 2, 3, 4) being the Stroh eigenvalues of the anisotropic piezoelectric material (Pan, 2004).

Similarly for I_z, its integration on each line segment in the anisotropic piezoelectric full plane can be expressed as

Table 2
Induced electric displacement component D_x (10^{-3} C/m^2) in both the circular inclusion and matrix of GaAs (001). The circular inclusion has a radius r = 10nm and the eigenstrain inside is linear in x-direction, i.e., $\gamma^{*0}_{Lm}=0$, $\gamma^{*x}_{xx}=\gamma^{*x}_{zz}=0.07$, $\gamma^{*z}_{Lm}=0$. The circle is approximated by the N-sided polygon (N = 10, 20, 40, 60, 80, and 100).

X = Z (nm)	N = 10	N = 20	N = 40	N = 60	N = 80	N = 100
1	0.39220	0.39073	0.39073	0.39072	0.39073	0.39072
2	0.77960	0.78145	0.78146	0.78144	0.78145	0.78145
3	1.16692	1.17201	1.17218	1.17215	1.17216	1.17218
4	1.56163	1.56171	1.56288	1.56281	1.56283	1.56292
5	1.95112	1.94755	1.95365	1.95334	1.95341	1.95364
6	2.29615	2.31788	2.34698	2.34280	2.34354	2.34412
7	7.69050	8.33241	3.05932	2.63476	2.80054	2.70166
8	6.65131	7.03739	7.18099	7.19186	7.20097	7.20496
9	5.91331	6.21443	6.29966	6.31281	6.31877	6.32141
10	5.37885	5.64181	5.70984	5.72156	5.72660	5.72875
11	4.95341	5.19221	5.25249	5.26316	5.26769	5.26959
12	4.59778	4.81863	4.87409	4.88399	4.88817	4.88990
13	4.29218	4.49856	4.55040	4.55968	4.56358	4.56519
14	4.02506	4.21923	4.26806	4.27680	4.28048	4.28198
15	3.78887	3.97240	4.01862	4.02690	4.03038	4.03180
16	3.57825	3.75235	3.79624	3.80410	3.80741	3.80875

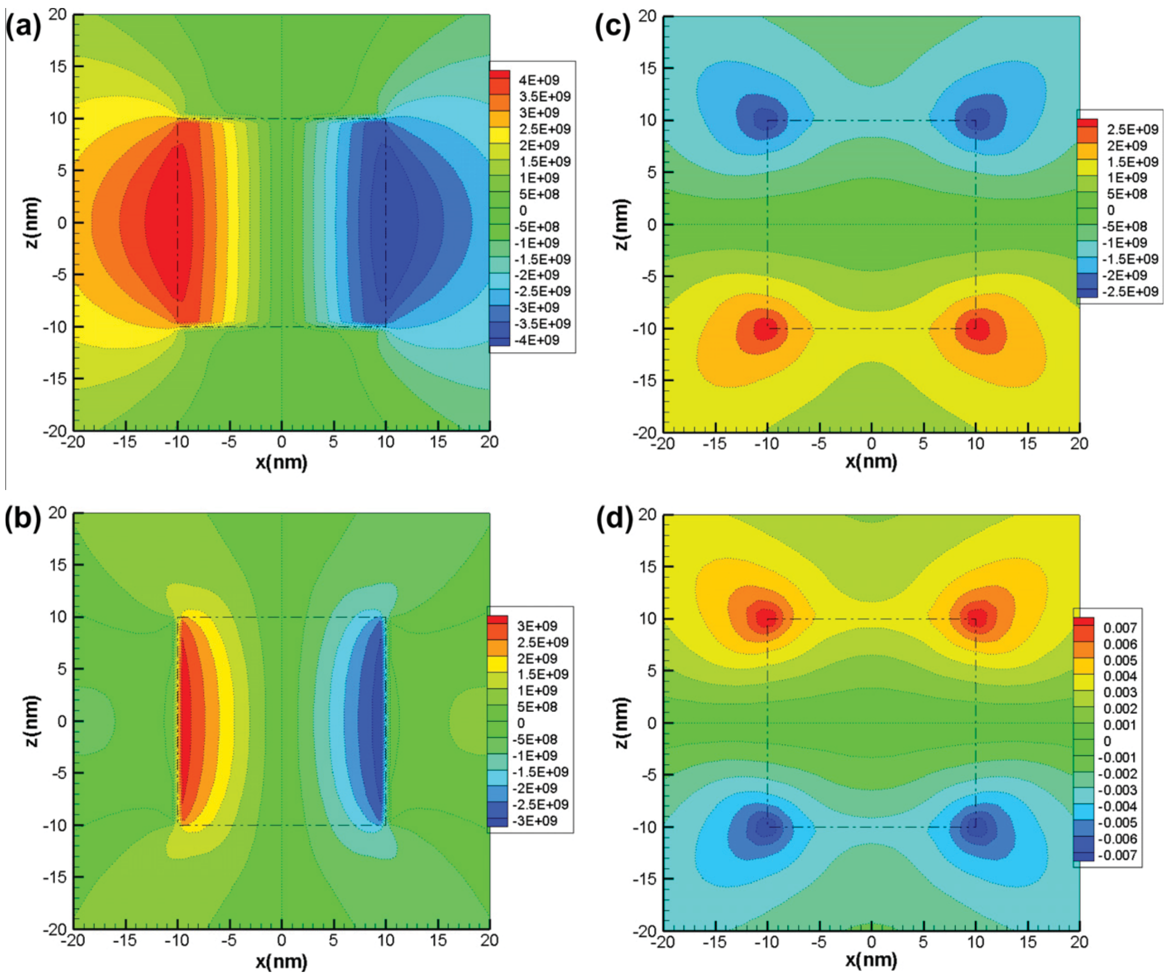

Fig. 2. A square QWR with eigenstrain $\gamma^{*0}_{Lm} = 0, \gamma^{*x}_{xx} = \gamma^{*x}_{zz} = 0.07, \gamma^{*z}_{Lm} = 0$ in GaAs (001) substrate: (a) the contour of stress σ_{xx} in N/m^2, (b) the contour of stress σ_{zz}, (c) the contour of stress σ_{xz}, (d) the contour of electric displacement D_z in C/m^2.

$$I_z(\boldsymbol{X}) = n_i \frac{l}{\pi} \mathrm{Im}\{A_{JR} h^z_R(X,Z) A_{KR}\} \tag{25}$$

where

$$\begin{aligned} h^z_R(X,Z) &= \int_0^1 \ln(z_R - s_R) z \, dt \\ &= \frac{z_2 - z_1}{4a^2}[a(2b-a) - 2(b^2 - a^2)\ln(a+b) + 2b^2 \\ &\quad \times \ln(b)] + \frac{z_1}{a}[-a + (a+b)\ln(a+b) - b\ln(b)] \end{aligned} \tag{26}$$

and its derivatives are

$$\begin{aligned} \frac{\partial h^z_R(X,Z)}{\partial X} &= -\frac{z_2 - z_1}{a^2}[a - b\ln(\tfrac{a+b}{b})] - \frac{z_1}{a}\ln(\tfrac{a+b}{b}) \\ \frac{\partial h^z_R(X,Z)}{\partial Z} &= -\frac{(z_2 - z_1)p_R}{a^2}[a - b\ln(\tfrac{a+b}{b})] - \frac{z_1 p_R}{a}\ln(\tfrac{a+b}{b}) \end{aligned} \tag{27}$$

We now derive the analytical expressions of J_x and J_z along a straight line segment. First, we need the integration of the full-plane Green's function. Recalling the following expression for the full-plane Green's function (Pan, 2004)

$$\begin{aligned} u^K_J(\boldsymbol{x}, \boldsymbol{X}) &= \frac{1}{\pi}\mathrm{Im}\{A_{JR}\ln(z_R - s_R)A_{KR}\} \\ &= \frac{1}{\pi}\mathrm{Im}\{A_{JR}\ln(p_R z + x - s_R)A_{KR}\} \end{aligned} \tag{28}$$

and integrating it with respect to x, we have

$$U^{xK}_J(\boldsymbol{x}, \boldsymbol{X}) = \frac{1}{\pi}\mathrm{Im}\left\{A_{JR}\left[-x + \frac{b_1\ln(a_1 x + b_1)}{a_1} + x\ln(a_1 x + b_1)\right]A_{KR}\right\} \tag{29}$$

where

$$\begin{aligned} a_1 &= 1 \\ b_1 &= p_R z - s_R \end{aligned} \tag{30}$$

Similarly, we have

$$U^{zK}_J(\boldsymbol{x}, \boldsymbol{X}) = \frac{1}{\pi}\mathrm{Im}\left\{A_{JR}\left[-z + \frac{b_2\ln(a_2 z + b_2)}{a_2} + z\ln(a_2 z + b_2)\right]A_{KR}\right\} \tag{31}$$

with

$$\begin{aligned} a_2 &= p_R \\ b_2 &= x - s_R \end{aligned} \tag{32}$$

Thus, integration of Eqs. (29) and (31) along the straight line segment gives us

$$J_x(\boldsymbol{X}) = n_x \frac{l}{\pi}\mathrm{Im}\{A_{JR} H^x_R(X,Z) A_{KR}\} \tag{33}$$

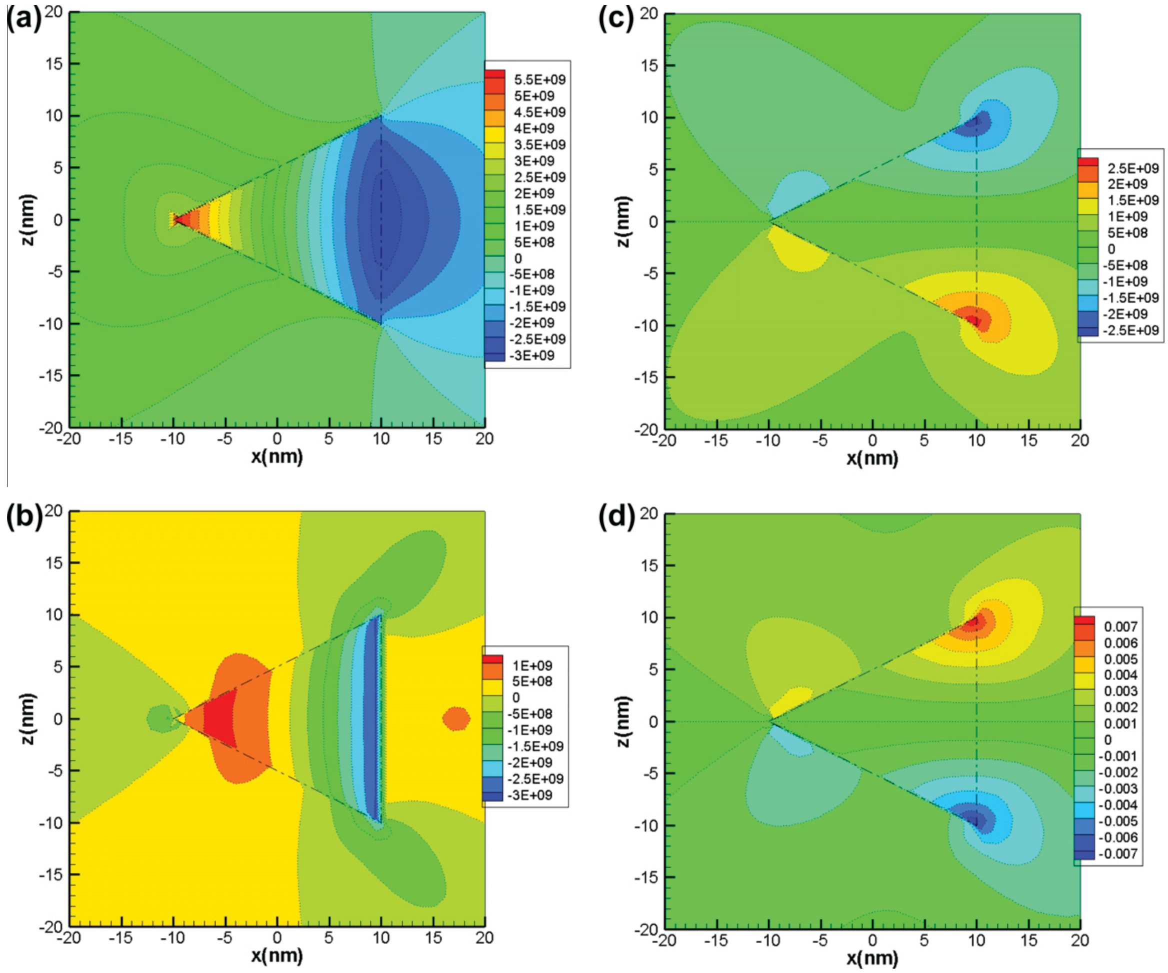

Fig. 3. A triangle QWR with eigenstrain $\gamma_{Lm}^{*0} = 0, \gamma_{xx}^{*x} = \gamma_{zz}^{*x} = 0.07, \gamma_{Lm}^{*z} = 0$ in GaAs (001) substrate: (a) the contour of stress σ_{xx}; (b) the contour of stress σ_{zz}; (c) the contour of stress σ_{xz}; (d) the contour of electric displacement D_z.

$$J_z(\boldsymbol{X}) = n_z \frac{l}{\pi} \mathrm{Im}\{A_{JR} H_R^z(X,Z) A_{KR}\} \tag{34}$$

where

$$\begin{aligned} H_R^x(X,Z) &= \int_0^1 \left[-x + \frac{b_1 \ln(a_1 x + b_1)}{a_1} + x \ln(a_1 x + b_1) \right] dt \\ &= -\frac{x_2 + x_1}{2} + \frac{1}{4a} [2ab - a^2 - 2(b^2 - a^2) \ln(a+b) \\ &\quad + 2b^2 \ln(b)] + \frac{b}{a} [-a + (a+b) \ln(a+b) - b \ln(b)] \end{aligned} \tag{35}$$

and its derivatives are

$$\begin{aligned} \frac{\partial H_R^x(X,Z)}{\partial X} &= \frac{-1}{a} \{a \ln(a+b) + b \ln(\tfrac{a+b}{b}) - b\} \\ \frac{\partial H_R^x(X,Z)}{\partial Z} &= \frac{-p_R}{a} \{a \ln(a+b) + b \ln(\tfrac{a+b}{b}) - b\} \end{aligned} \tag{36}$$

Similarly we also have

$$\begin{aligned} H_R^z(X,Z) &= \int_0^1 [-z + \frac{b_2 \ln(a_2 z + b_2)}{a_2} + z \ln(a_2 z + b_2)] dt \\ &= -\frac{z_2 + z_1}{2} + \frac{1}{4ap_R} [2ab - a^2 - 2(b^2 - a^2) \ln(a+b) \\ &\quad + 2b^2 \ln(b)] + \frac{b}{ap_R} [-a + (a+b) \ln(a+b) - b \ln(b)] \end{aligned} \tag{37}$$

and its derivatives

$$\begin{aligned} \frac{\partial H_R^z(X,Z)}{\partial X} &= \frac{-1}{ap_R} \{a \ln(a+b) + b \ln(\tfrac{a+b}{b}) - b\} \\ \frac{\partial H_R^z(X,Z)}{\partial Z} &= \frac{-1}{a} \{a \ln(a+b) + b \ln(\tfrac{a+b}{b}) - b\} \end{aligned} \tag{38}$$

With the extended displacements and their derivatives, we can find immediately the elastic strain and electric fields from the following expressions

$$\gamma_{kp}(\boldsymbol{X}) = \frac{1}{2} \gamma_{Lm}^* C_{iJLm} \int_{\partial V} [u_{J,X_p}^k(\boldsymbol{x};\boldsymbol{X}) + u_{J,X_k}^p(\boldsymbol{x};\boldsymbol{X})] n_i(\boldsymbol{x}) \, \mathrm{d}S(\boldsymbol{x}); \quad k,p = 1,2,3 \tag{39a}$$

$$E_p(X) = -\gamma_{Lm}^* C_{iJLm} \int_{\partial V} u_{J,X_p}^4(x;X) n_i(x) \, \mathrm{d}S(x); \;\; p = 1,2,3 \tag{39b}$$

The stresses and electric displacements are obtained from strains and electric fields via the coupled constitutive relation (Pan, 2004).

In summary, therefore, we have derived the exact closed-form solutions for the elastic and piezoelectric fields induced by an arbitrary polygonal inclusion with linear eigenstrains. Since our result is in an exact-closed form, solutions to multiple inclusions can be simply derived by superposing the contributions from all inclu-

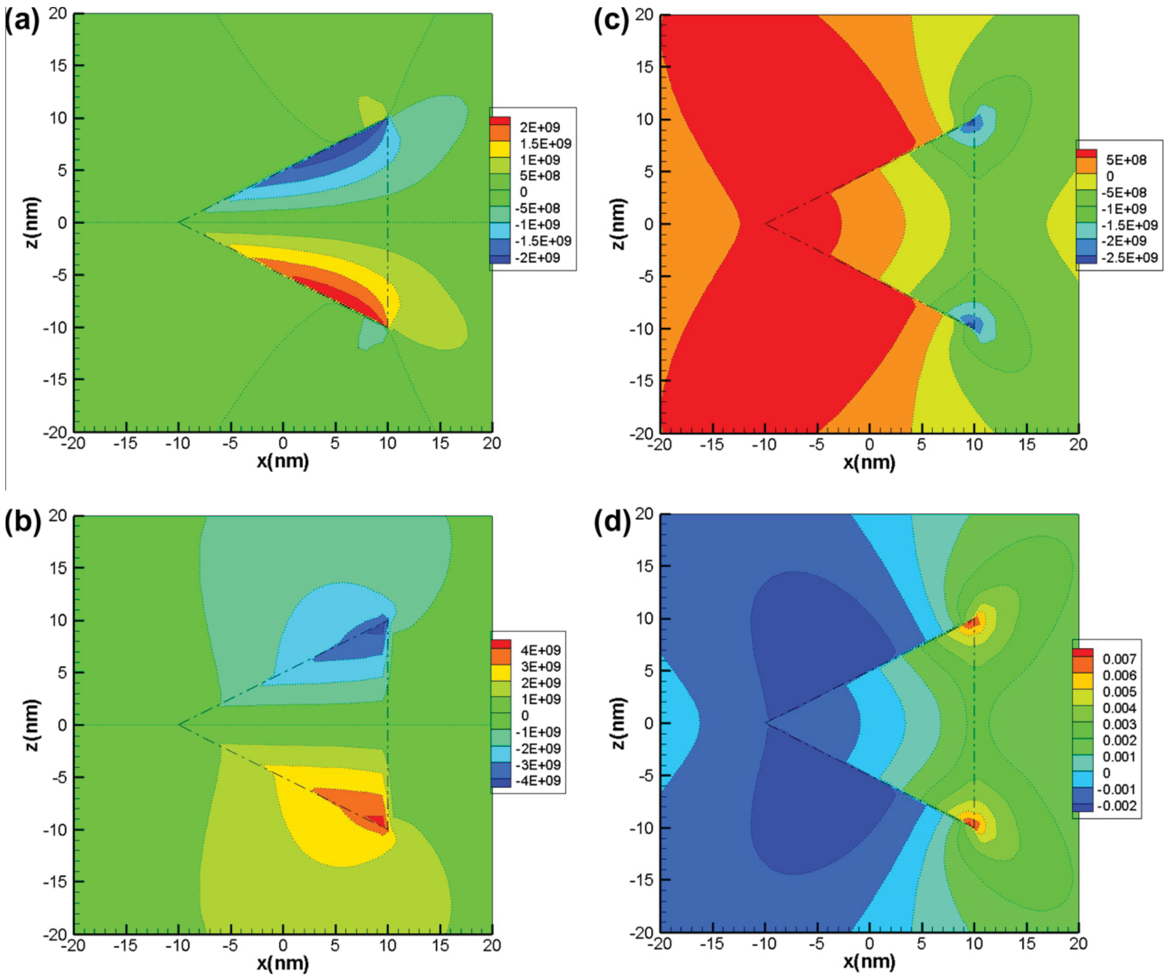

Fig. 4. A triangle QWR with eigenstrain $\gamma^{*0}_{Lm}=0, \gamma^{*x}_{Lm}=0, \gamma^{*z}_{xx}=\gamma^{*z}_{zz}=0.07$ in GaAs (001) substrate: (a) the contour of stress σ_{xx}; (b) the contour of stress σ_{zz}; (c) the contour of stress σ_{xz}; (d) the contour of electric displacement D_z.

sions. This is particularly useful in the analysis of QWR-array induced elastic and piezoelectric fields (Glas, 2002a,b).

We remark that the solutions presented in this paper are for the general anisotropic and piezoelectric 2D linear eigenstrain problem. It is worth emphasizing that our results include the general anisotropic elastic case and the uniform eigenstrain case in general anisotropic piezoelectric 2D domain (Pan, 2004) as the special cases.

To test the accuracy of our solutions, we assume that the piezoelectric full plane is made of GaAs (001), with an inclusion of circular QWR of radius $r = 10$ nm. We further assume that within the circle, there is a linear eigenstrain distribution $\gamma^{*0}_{Lm}=0$, $\gamma^{*x}_{xx}=\gamma^{*x}_{zz}=0.07$ (the other components $\gamma^{*x}_{Lm}=0$), $\gamma^{*z}_{Lm}=0$ (thereafter, we only study the hydrostatic linear eigenstrain in x or in z). The elastic properties for GaAs (001) are $C_{11} = 118 \times 10^9$ N/m^2, $C_{12} = 54 \times 10^9$ N/m^2, and $C_{44} = 59 \times 10^9$ N/m^2, and piezoelectric constant and relative permeability are, respectively, $e_{14} = -16 \times 10^{-9}$ C/m^2 and $\varepsilon_r = 12.5$ (Pan, 2002b). We point out that, for GaAs (001), the global coordinates x, y, and z are coincident with the crystalline axes [100], [010], and [001]. In our calculation, we approximate the curved circle with N piecewise straight-line segments. Namely, we replace the circle with an N-sided regular polygon, for N equals 10, 20, 40, 60, 80, and 100. The induced stresses and electric displacements along the diagonal line of the circle ($X = Z$) are listed in Tables 1 and 2 for the polygon with different side N. Notice that points $X = Z = 1$ nm to 7 nm are inside the circular QWR, whilst $X = Z = 8$ nm to 16 nm are points in the substrate (or matrix).

From Tables 1 and 2, it is obvious that for any fixed point, the induced field quantities within the circular inclusion and in the matrix both converge with increasing N. It is further noticed that these field quantities converge faster at points near the center than those far from the center. Especially for points close to the interface between the inclusion and matrix, the convergence becomes slow. For instance, the point $X = Z = 7$ nm experiences the slowest convergence rate among other points because it is the closest point to the boundary of the circle ($X = Z = 7.07$ nm). We have also checked the stresses and electric displacements both in the inclusion and matrix induced by different linear eigenstrain distribution and found that they all converge when N is large.

3. Numerical examples

We now apply the exact closed-form solutions to the QWR made of different shapes. We first consider a square QWR (20 nm $\times$ 20 nm) in piezoelectric GaAs (001) with three different eigenstrain distributions: Case #1 with a linear eigenstrain in x ($\gamma^{*0}_{Lm}=0$, $\gamma^{*x}_{xx}=\gamma^{*x}_{zz}=0.07$, $\gamma^{*z}_{Lm}=0$); Case #2 with a linear eigen-

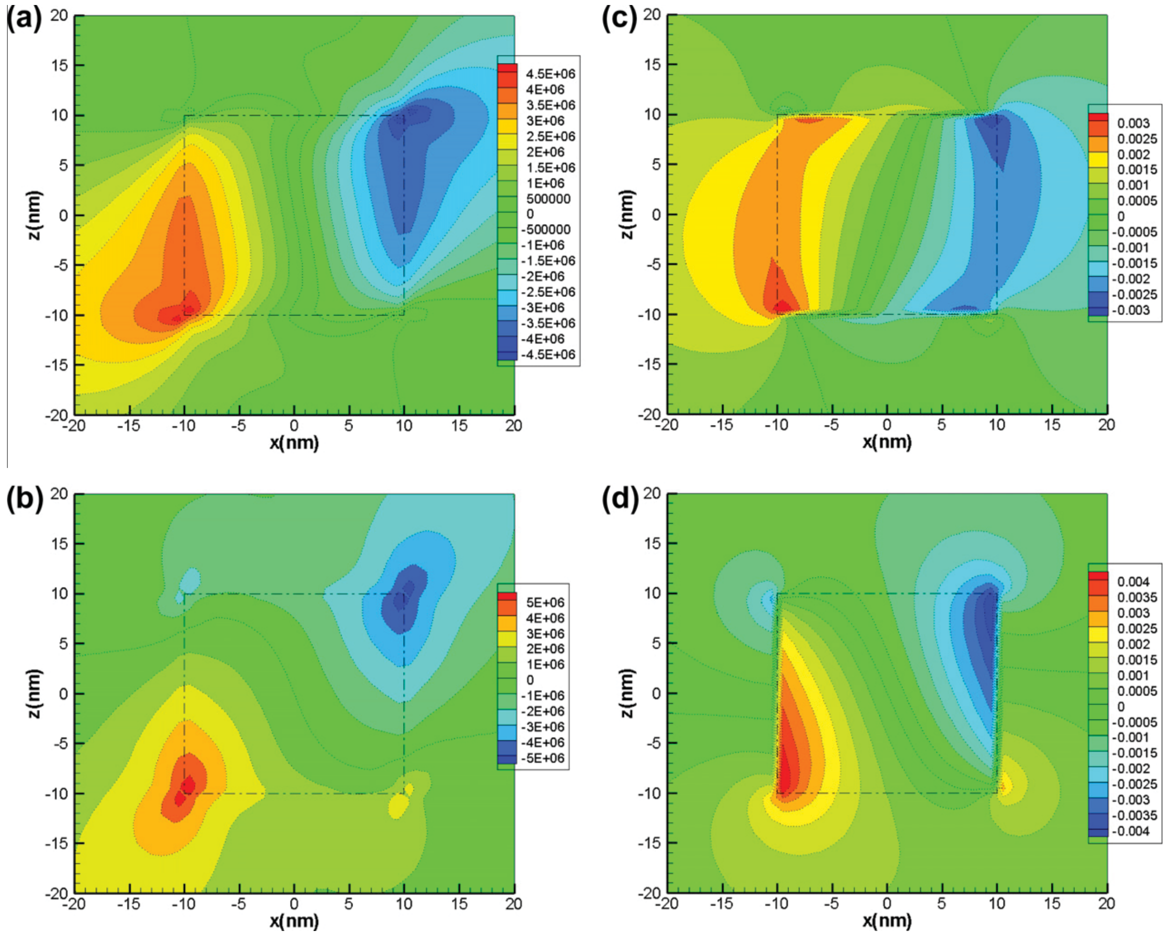

Fig. 5. A square QWR with eigen-electric field $-E_x^{*x} = -E_z^{*x} = 0.07$ V/m in GaAs (001) substrate: (a) the contour of stress σ_{xy}; (b) the contour of stress σ_{yz}; (c) the contour of electric displacement D_x; (d) the contour of electric displacement D_z.

strain in z ($\gamma_{Lm}^{*0} = 0$, $\gamma_{Lm}^{*x} = 0$, $\gamma_{xx}^{*z} = \gamma_{zz}^{*z} = 0.07$); and Case #3 with a linear eigenstrain in both x and z ($\gamma_{Lm}^{*0} = 0$, $\gamma_{xx}^{*x} = \gamma_{zz}^{*x} = 0.07$, $\gamma_{xx}^{*z} = \gamma_{zz}^{*z} = 0.07$).

Shown in Fig. 2a and b are, respectively, the contours of the stresses σ_{xx} and σ_{zz}, and in Fig. 2c and d, respectively, the contours of the stress σ_{xz} and electric displacement D_z, due to a hydrostatic linear eigenstrain in x (Case #1). The location of the square is also shown by dashed lines. Some interesting features can be observed from these figures: (1) The distributions of the induced stress and electric displacement field clearly show certain symmetry with respect to the x- and z-axes. This is due to the fact that the inclusion is square shape and the material is cubic. (2) The induced stresses σ_{xx} and σ_{zz} show clearly the linear variation in x within the square QWR, with their maximum magnitudes being at $x = \pm 10$ nm, i.e., at the left and right sides of the square. (3) The features of stress σ_{xz} and electric displacement D_z (Fig. 2c and d) are exactly the same except for their magnitudes. This is further related to the cubic property of the material and the square shape of the inclusion. Four concentrations can be observed at the four corners of the square for σ_{xz} and D_z. (4) Different to the uniform eigenstrain case, the induced field quantities by the linear eigenstrain are mostly continuous across the boundary of the inclusion. This is particularly true for the extended tractions where they remain continuously across the inclusion boundary. This actually partially verifies the accuracy of our analytical solutions to a certain extent.

Fig. 3a–d show the corresponding contours of stresses (σ_{xx}, σ_{zz}, σ_{xz}) and electric displacement (D_z), due to an isosceles triangular inclusion with all side length of 20 nm within the GaAs (001) substrate, under a hydrostatic linear eigenstrain in x ($\gamma_{Lm}^{*0} = 0, \gamma_{xx}^{*x} = \gamma_{zz}^{*x} = 0.07, \gamma_{Lm}^{*z} = 0$). The corresponding results due to a hydrostatic linear eigenstrain in z are shown in Fig. 4a–d. Comparing Fig. 3a–d to Fig. 2a–d under a hydrostatic linear eigenstrain in x, it is observed that the induced field depends strongly on the shape of the inclusion (square vs. triangle) and that there is an apparent concentration at the left corner of the triangular inclusion (Fig. 3a and b). Comparing Fig. 3a–d to Fig. 4a–d for the same triangular inclusion but under different linear eigenstrain (linear in x vs. linear in z), it is seen that for the hydrostatic linear eigenstrain in z, there is an obvious non-uniform gradient inside the triangle for the shear stress and electric displacement (Fig. 4c and d) since contours are curved there.

Then we would like to study the stress and electric displacement distributions under a linear eigen-electric field. We calculate the square and triangle model as above, with the linear eigen-electric field $-E_x^{*x} = -E_z^{*x} = 0.07$ V/m, along x-direction. Shown in Fig. 5a–d and Fig. 6a–d are the contours of the stress σ_{xy}, σ_{yz}.and the electric displacement D_x, D_z respectively for square and triangle model. Observing the square model, we find that the distribution fields for stress and electric displacement are all anti-centrosymmetric, shown in Fig. 5a–d. However, for triangle model, the stress and electric displacement distributions don't show any symmetry

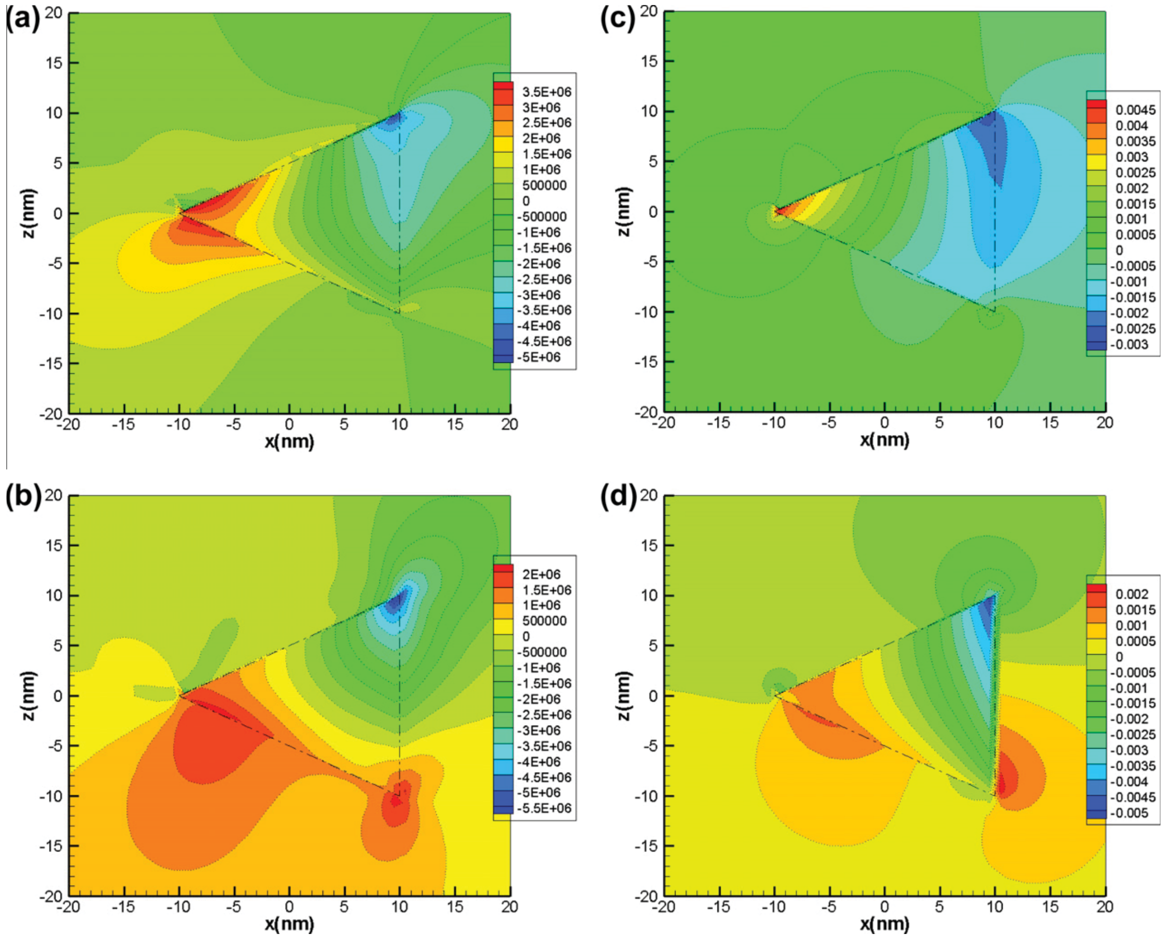

Fig. 6. A triangle QWR with eigen-electric field $-E_x^{*x} = -E_z^{*x} = 0.07$ V/m in GaAs (001) substrate: (a) the contour of stress σ_{xy}; (b) the contour of stress σ_{yz}; (c) the contour of electric displacement D_x; (d) the contour of electric displacement D_z.

(Fig. 6a–d). After analyzing on results, we find that only when the direction of the linear distribution of eigenstrain or eigen-electric field is vertical to the symmetric axis of the polygon, the results satisfy the symmetry. For instance, if we give eigenstrain or eigen-electric field along z-direction for triangle model, the results satisfy some kind of symmetry (Fig. 4a and b). Furthermore, we find that in our results, the normal stresses σ_{xx} and σ_{zz} vanish in both square and triangle cases.

For a special circumstance where the average eigenstrain is zero in the QWR, we would like to see the mean of the induced strain field (or stress field), which is defined as

$$\bar{u}_{K,p} = \frac{1}{V}\int_V u_{K,p}(X)\,\mathrm{d}V(X) \tag{40}$$

Then we also consider this case for both square and triangle model. After calculation, we find that for square model, no matter the linear eigenstrain is along x or z-direction, which means the average eigenstrain in the QWR is zero, the mean of the induced stress field is zero for both the interior and exterior field. This can be visually observed in Fig. 2a–d. However, for triangle model, to ensure the average eigenstrain is zero, we can only assume the linear eigenstrain is along z-direction for our model. Then we also calculate the mean of the induced stress field. We find $\bar{\sigma}_{xx}$ and $\bar{\sigma}_{zz}$ are zero, but $\bar{\sigma}_{xz}$ is not zero. These results can also be observed in Fig. 2a–c. Furthermore, we obtain the mean of stress $\bar{\sigma}_{xz} = 0.071$ GPa for our triangle inclusion system. The results above are useful to analyze the properties of polygonal inclusion problem.

To further investigate the features of the linear eigenstrain induced fields, we plot their variations along different directions. We first consider the non-polygonal inclusion case. A circular ($r = 10$ nm) and an elliptical (semi-major and semi-minor axes are 20nm and 10nm) inclusion in GaAs (001) substrate. For these two cases, we approximate the smooth boundary by the N-sided polygon with $N = 100$. We are interested in the variation of the induced stress and electric displacement along the x-axis, z-axis and 45-degree to the x-direction ($x = z$) due to linear eigenstrain in x or z, and simultaneously in both x and z. Shown in Fig. 7a–f are the results for the circular inclusion and in Fig. 8a–f those for the elliptical inclusion. There are three curves in each figure, and the field variation includes points both inside and outside the QWR.

It is observed from Fig. 7a–d that, for linear eigenstrain in x, the variation of stress σ_{xx} along x-axis and the diagonal line $x = z$ is a linear function of x, whilst the variation of electric displacement D_z along z-axis and $z = x$ is a linear function of z. It is further seen from these figures that the traction and the normal electric displacement are continuous cross the interface between the QWR and substrate either along the x-axis or z-axis. We remark that along x-axis, the interface is at $x = 10$ nm, and along the diagonal line $x = z$, the interface is at $x = z = 7.07$ nm. The variation of the stress and electric dis-

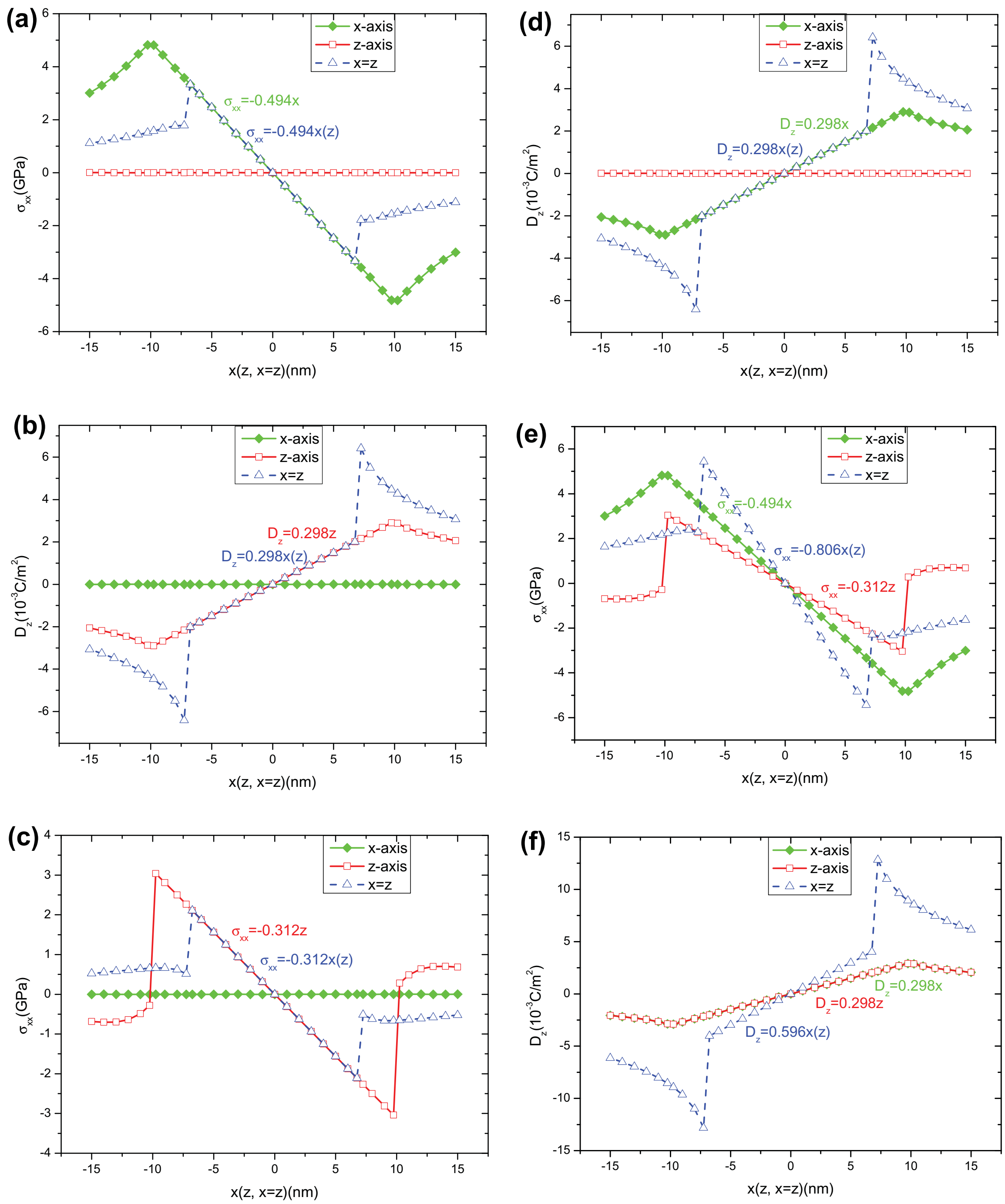

Fig. 7. The variation of stress σ_{xx} and electric displacement D_z along x-axis, z-axis and 45-degree to the x-direction under linear eigenstrain within a circular QWR which is embedded in GaAs (001) substrate. (a) σ_{xx} under linear eigenstrain $\gamma^{*0}_{Lm} = 0, \gamma^{*x}_{xx} = \gamma^{*x}_{zz} = 0.07, \gamma^{*z}_{Lm} = 0$. (b) D_z under linear eigenstrain $\gamma^{*0}_{Lm} = 0, \gamma^{*x}_{xx} = \gamma^{*x}_{zz} = 0.07, \gamma^{*z}_{Lm} = 0$. (c) σ_{xx} under linear eigenstrain $\gamma^{*0}_{Lm} = 0, \gamma^{*x}_{Lm} = 0, \gamma^{*z}_{xx} = \gamma^{*z}_{zz} = 0.07$. (d) D_z under linear eigenstrain $\gamma^{*0}_{Lm} = 0, \gamma^{*x}_{Lm} = 0, \gamma^{*z}_{xx} = \gamma^{*z}_{zz} = 0.07$. (e) σ_{xx} under linear eigenstrain $\gamma^{*0}_{Lm} = 0, \gamma^{*x}_{xx} = \gamma^{*x}_{zz} = 0.07, \gamma^{*z}_{xx} = \gamma^{*z}_{zz} = 0.07$. (f) D_z under linear eigenstrain $\gamma^{*0}_{Lm} = 0, \gamma^{*x}_{xx} = \gamma^{*x}_{zz} = 0.07, \gamma^{*z}_{xx} = \gamma^{*z}_{zz} = 0.07$.

placement along x-axis, z-axis, and 45 degree to x-axis due to the combined linear eigenstrain in x and z can be obtained by the method of superposition, which is shown in Fig. 7e–f.

It is further noticed from Fig. 7a–f that along x-axis or z-axis, the induced stress or electric displacement could be identically zero due to the symmetry of the material property and the circular QWR shape, and that the maximum values of the nonzero components are on the interface.

Fig. 8a–f show the corresponding variations of the stress and electric displacement along the three directions (x-axis, z-axis, and line $x = z$) due to an elliptical QWR under linear eigenstrains. It is pointed out that the interface along $x = z$ is at $x = z = 8.9$ nm. While the variation of these fields is similar to that in Fig. 7a–f, we notice that, along certain direction, the maximum D_z could be located outside the QWR. For instance for the electric displacement along $x = z$, the maximum is reached in the substrate slightly outside the QWR.

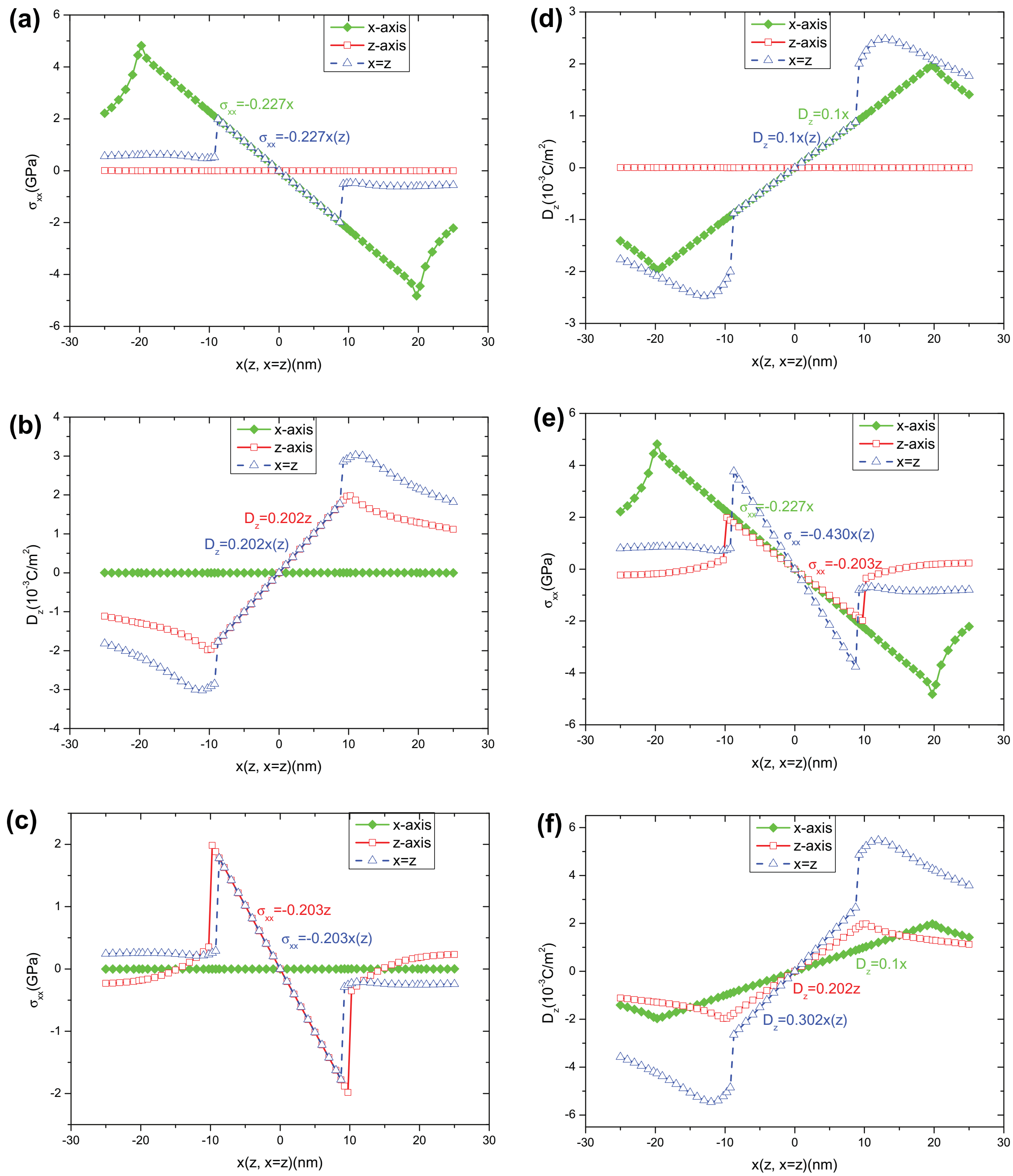

Fig. 8. The variation of stress σ_{xx} and electric displacement D_z along x-axis, z-axis and 45-degree to the x-direction under linear eigenstrain within an elliptical QWR which is embedded in GaAs (001) substrate. (a) σ_{xx} under linear eigenstrain $\gamma^{*0}_{Lm}=0, \gamma^{*x}_{xx}=\gamma^{*x}_{zz}=0.07, \gamma^{*z}_{Lm}=0$. (b) D_z under linear eigenstrain $\gamma^{*0}_{Lm}=0, \gamma^{*x}_{xx}=\gamma^{*x}_{zz}=0.07, \gamma^{*z}_{Lm}=0$. (c) σ_{xx} under linear eigenstrain $\gamma^{*0}_{Lm}=0, \gamma^{*x}_{Lm}=0, \gamma^{*z}_{xx}=\gamma^{*z}_{zz}=0.07$. (d) D_z under linear eigenstrain $\gamma^{*0}_{Lm}=0, \gamma^{*x}_{Lm}=0, \gamma^{*z}_{xx}=\gamma^{*z}_{zz}=0.07$. (e) σ_{xx} under linear eigenstrain $\gamma^{*0}_{Lm}=0, \gamma^{*x}_{xx}=\gamma^{*x}_{zz}=0.07, \gamma^{*z}_{xx}=\gamma^{*z}_{zz}=0.07$. (f) D_z under linear eigenstrain $\gamma^{*0}_{Lm}=0, \gamma^{*x}_{xx}=\gamma^{*x}_{zz}=0.07, \gamma^{*z}_{xx}=\gamma^{*z}_{zz}=0.07$.

In summary, for the circular and elliptical inclusion with linear eigenstrain in x and z, our results show that the stress and electric displacement inside the inclusion is linear function of x and z. However, should the inclusion is in other shape, such linear-dependent feature disappear. This is illustrated in Figs. 9 and 10, respectively, for the square and triangular inclusion case. The square and triangle are oriented, respectively, the same way as in Figs. 2 and 3. First, it is noted from Fig. 9a–f that under linear eigenstrain in either x or z, the stress and electric displacement is no longer linear along the diagonal direction $x = z$. For the triangular case, all the lines inside the inclusion become nonlinear, except for σ_{xx} along z-axis due to the linear eigenstrain in z as shown in Fig. 10c. It is further noticed that due to the geometric shape of the triangle, the x- and/or z-axis is no longer the line of symmetry. In other words, along these axes, the field quantities may not be zero any more (Fig. 10a, d, e and f). These phenomena are new and should be important for us to understand the properties for inclusion problems with graded eigenstrain.

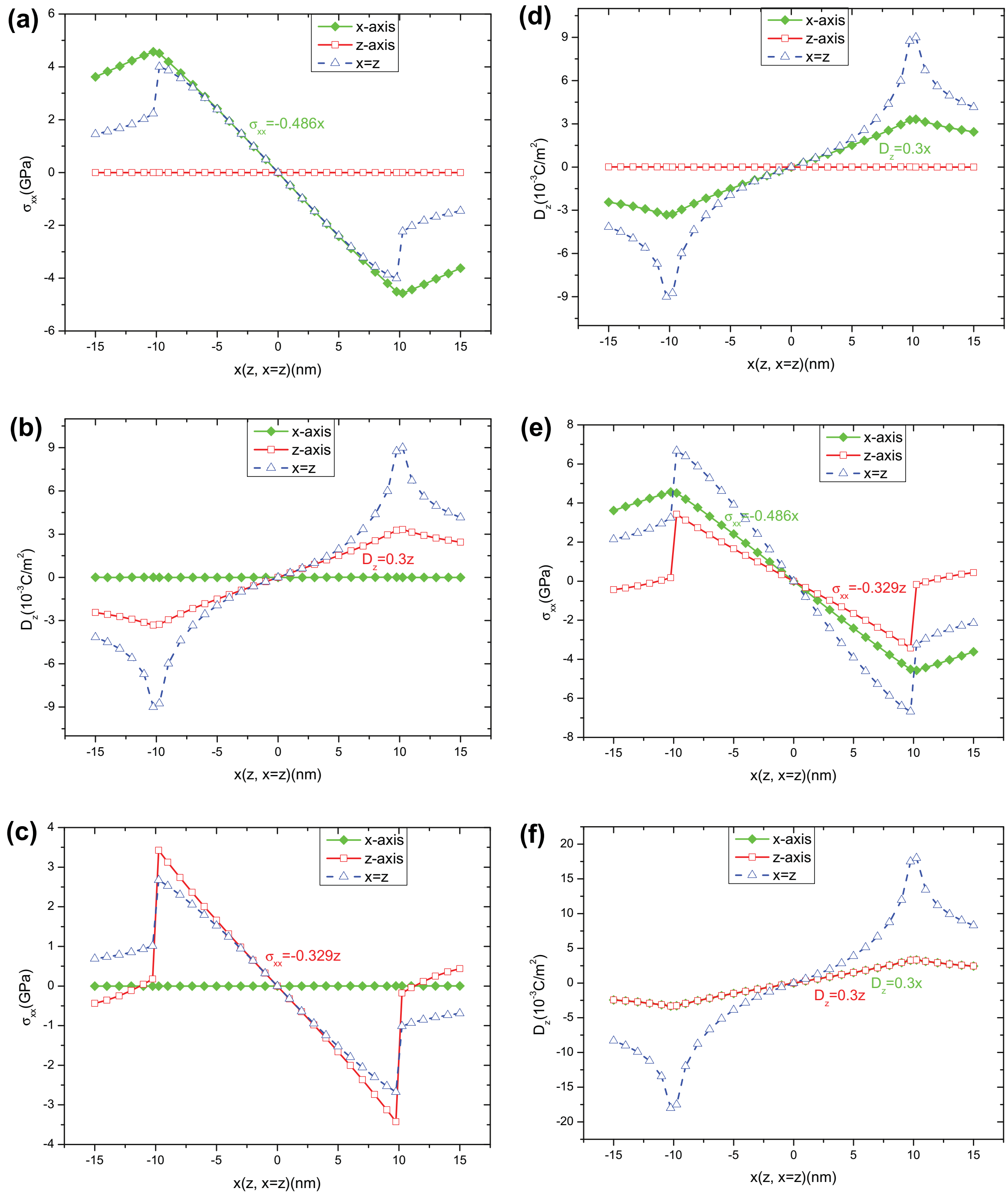

Fig. 9. The variation of stress σ_{xx} and electric displacement D_z along x-axis, z-axis and 45-degree to the x-direction under linear eigenstrain within a square QWR which is embedded in GaAs (001) substrate. (a) σ_{xx} under linear eigenstrain $\gamma_{Lm}^{*0} = 0, \gamma_{xx}^{*x} = \gamma_{zz}^{*x} = 0.07, \gamma_{Lm}^{*z} = 0$. (b) D_z under linear eigenstrain $\gamma_{Lm}^{*0} = 0, \gamma_{xx}^{*x} = \gamma_{zz}^{*x} = 0.07, \gamma_{Lm}^{*z} = 0$. (c) σ_{xx} under linear eigenstrain $\gamma_{Lm}^{*0} = 0, \gamma_{Lm}^{*x} = 0, \gamma_{xx}^{*z} = \gamma_{zz}^{*z} = 0.07$. (d) D_z under linear eigenstrain $\gamma_{Lm}^{*0} = 0, \gamma_{Lm}^{*x} = 0, \gamma_{xx}^{*z} = \gamma_{zz}^{*z} = 0.07$. (e) σ_{xx} under linear eigenstrain $\gamma_{Lm}^{*0} = 0, \gamma_{xx}^{*x} = \gamma_{zz}^{*x} = 0.07, \gamma_{xx}^{*z} = \gamma_{zz}^{*z} = 0.07$. (f) D_z under linear eigenstrain $\gamma_{Lm}^{*0} = 0, \gamma_{xx}^{*x} = \gamma_{zz}^{*x} = 0.07, \gamma_{xx}^{*z} = \gamma_{zz}^{*z} = 0.07$.

4. Conclusions

In this paper, we have derived an exact closed-form solution for the Eshelby problem of arbitrarily shaped inclusions in an anisotropic piezoelectric full plane. The eigenstrain field inside the inclusion is assumed to be linear functions of x and z. Based on the equivalent body-force concept of eigenstrain, we expressed the induced elastic and piezoelectric fields in terms of a line integral on the boundary of the inclusion with the integrand being the line-source Green's function. Using the exact closed-form Green's function, the line integral was carried out analytically by assuming a piecewise straight-line boundary for the inclusion,

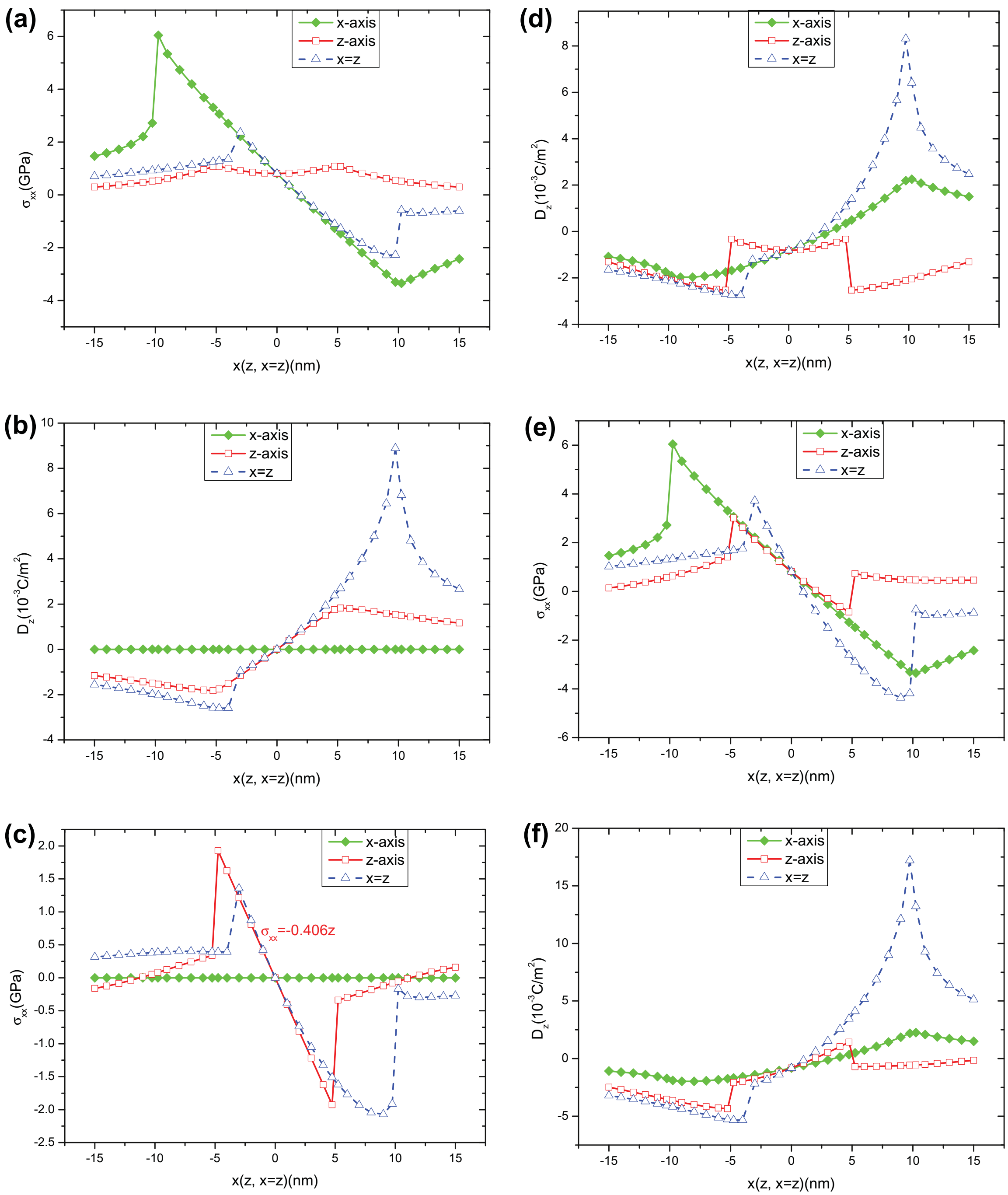

Fig. 10. The variation of stress σ_{xx} and electric displacement D_z along x-axis, z-axis and 45-degree to the x-direction under linear eigenstrain within a triangular QWR which is embedded in GaAs (001) substrate. (a) σ_{xx} under linear eigenstrain $\gamma_{Lm}^{*0} = 0, \gamma_{xx}^{*x} = \gamma_{zz}^{*x} = 0.07, \gamma_{Lm}^{*z} = 0$. (b) D_z under linear eigenstrain $\gamma_{Lm}^{*0} = 0, \gamma_{xx}^{*x} = \gamma_{zz}^{*x} = 0.07, \gamma_{Lm}^{*z} = 0$. (c) σ_{xx} under linear eigenstrain $\gamma_{Lm}^{*0} = 0, \gamma_{Lm}^{*x} = 0, \gamma_{xx}^{*z} = \gamma_{zz}^{*z} = 0.07$. (d) D_z under linear eigenstrain $\gamma_{Lm}^{*0} = 0, \gamma_{Lm}^{*x} = 0, \gamma_{xx}^{*z} = \gamma_{zz}^{*z} = 0.07$. (e) σ_{xx} under linear eigenstrain $\gamma_{Lm}^{*0} = 0, \gamma_{xx}^{*x} = \gamma_{zz}^{*x} = 0.07, \gamma_{xx}^{*z} = \gamma_{zz}^{*z} = 0.07$. (f) D_z under linear eigenstrain $\gamma_{Lm}^{*0} = 0, \gamma_{xx}^{*x} = \gamma_{zz}^{*x} = 0.07, \gamma_{xx}^{*z} = \gamma_{zz}^{*z} = 0.07$.

i.e., an arbitrarily shaped polygon. The solution is then applied to a square, a triangle, a circle and an ellipse QWR within the GaAs (001) substrate, with results clearly showing the importance of linear eigenstrain, as compared to the uniform eigenstrain case. Our numerical results can also be served as benchmarks and could be useful to the analysis of strained QWR structures with arbitrarily shaped cross-section and with general anisotropic piezoelectricity.

Acknowledgements

This work is supported by the National Natural Science Foundation of China (Nos. 10772106, 11072138, 11172273), Shanghai Leading Academic Discipline Project (No. S30106) and the Research Fund for the Doctoral Program of Higher Education of China (No. 20113108110005). The authors are very grateful to both reviewers for their valuable comments and constructive suggestions.

References

Andreev, A.D., Downes, J.R., Faux, D.A., O'Reilly, E.P., 1999. Strain distribution in quantum dots of arbitrary shape. J. Appl. Phys. 86, 297–305.

Chu, H.J., Pan, E., Ramsey, J.J., Wang, J., Xue, C.X., 2011. A general perturbation method for inhomogeneities in anisotropic and piezoelectric solids with applications to quantum-dot nanostructures. Int. J. Solids Struct. 48, 673–679.

Davies, J.H., 1998. Elastic and piezoelectric fields around a buried quantum dot: A simple picture. J. Appl. Phys. 84, 1358–1365.

Dong, C.Y., Lo, S.H., Cheung, Y.K., 2003. Stress analysis of inclusion problems of various shapes in an infinite anisotropic elastic medium. Comput. Meth. Appl. Mech. Eng. 192, 683–696.

Eshelby, J.D., 1957. The determination of the elastic field of an ellipsoidal inclusion, and related problems. Proc. R. Soc. Lond. A241, 376–396.

Eshelby, J.D., 1961. Elastic inclusions and inhomogeneities. In: Sneddon, I.N., Hill, R. (Eds.), Progress in Solid Mechanics, vol. 2. North-Holland, Amsterdam, pp. 89–140.

Freund, L.B., Gosling, T.J., 1995. Critical thickness for growth of strained quantum wires in substrate V-grooves. Appl. Phys. Lett. 66, 2822–2824.

Gao, X.L., Ma, H.M., 2010. Solution of Eshelby's inclusion problem with a bounded domain and Eshelby's tensor for a spherical inclusion in a finite spherical matrix based on a simplified strain gradient elasticity theory. J. Mech. Phys. Solids 58, 779–797.

Glas, F., 2002a. Analytical calculation of the strain field of single and periodic misfitting polygonal wires in a half-space. Philos. Mag. A82, 2591–2608.

Glas, F., 2002b. Elastic relaxation of isolated and interacting truncated pyramidal quantum dots and quantum wires in a half space. Appl. Surf. Sci. 188, 9–18.

Guo, L., Nie, G.H., Chan, C.K., 2011. Elliptical inhomogeneity with polynomial eigenstrains embedded in orthotropic materials. Arch. Appl. Mech. 81, 157–170.

Ju, J.W., Sun, L.Z., 2001. Effective elastoplastic behavior of metal matrix composites containing randomly located aligned spheroidal inhomogeneities. Part I: micromechanics-based formulation. Int. J. Solids Struct. 38, 183–201.

Kouris, D.A., Mura, T., 1989. The elastic field of a hemispherical inhomogeneity at the free surface of an elastic half space. J. Mech. Phys. Solids 37, 365–379.

Li, S., Sauer, R., Wang, G., 2005. A circular inclusion in a finite elastic domain. I. The Dirichelt–Eshelby problem. Acta Mechanica 179, 67–90.

Li, S., Sauer, R., Wang, G., 2007. The Eshelby tensors in a finite spherical domain: I. theoretical formulations. J. Appl. Mech. 74, 770–783.

Michelitsch, T.M., Gao, H., Levin, V.M., 2003. Dynamic Eshelby tensor and potentials for ellipsoidal inclusions. Proc. R. Soc. Lond. A459, 863–890.

Mura, T., 1987. Micromechanics of Defects in Solids, 2nd Revised Edition. Kluwer Academic Publishers, Dordrecht.

Nie, G.H., Guo, L., Chan, C.K., Shin, F.G., 2007. Non-uniform eigenstrain induced stress field in an elliptic inhomogeneity embedded in orthotropic media with complex roots. Int. J. Solids Struct. 44, 3575–3593.

Nozaki, H., Taya, M., 1997. Elastic fields in a polygon-shaped inclusion with uniform eigenstrains. J. Appl. Mech. 64, 495–502.

Pan, E., 2002a. Elastic and piezoelectric fields around a quantum dot: Fully coupled or semi-coupled model? J. Appl. Phys. 91, 3785–3796.

Pan, E., 2002b. Elastic and piezoelectric fields in substrates GaAs (001) and GaAs (111) due to a buried quantum dot. J. Appl. Phys. 91, 6379–6387.

Pan, E., 2004. Eshelby problem of polygonal inclusions in anisotropic piezoelectric full- and half-planes. J. Mech. Phys. Solids 52, 567–589.

Rahman, M., 2002. The isotropic ellipsoidal inclusion with a polynomial distribution of eigenstrain. J. Appl. Mech. 69, 593–601.

Rodin, G.J., 1996. Eshelby's inclusion problem for polygons and polyhedra. J. Mech. Phys. Solids 44, 1977–1995.

Ru, C.Q., 1999. Analytical solution for Eshelby's problem of an inclusion of arbitrary shape in a plane or half-plane. J. Appl. Mech. 66, 315–322.

Ru, C.Q., 2000. Eshelby's problem for two-dimensional piezoelectric inclusions of arbitrary shape. Proc. R. Soc. Lond. A456, 1051–1068.

Sharma, P., Sharma, R., 2003. On the Eshelby's inclusion problem for ellipsoids with nonuniform dilatational Gaussian and exponential eigenstrains. J. Appl. Mech. 70, 418–425.

Sun, L.G., Xu, K.Y., Pan, E., 2012. Irregular inhomogeneities in an anisotropic piezoelectric plane. J. Appl. Mech. 79, 021014.

Wang, J., Chu, H.J., 2006. A perturbation theory for calculating strain distributions in heterogeneous and anisotropic quantum dot structures. J. Appl. Phys. 100, 053520.

Yu, H.Y., Sanday, S.C., Chang, C.I., 1994. Elastic inclusion and inhomogeneities in transversely isotropic solids. Proc. R. Soc. Lond. A444, 239–252.

Zou, W., He, Q., Huang, M., Zheng, Q., 2010. Eshelby's problem of non-elliptical inclusions. J. Mech. Phys. Solids 58, 346–372.